Hexameric Polyoxotantalate with Proton Conduction Property

Hanhan Chen, Mingyang Zhang, Yuyan Li, Pengtao Ma, Jingping Wang,* and Jingyang Niu*

Henan Key Laboratory of Polyoxometalate Chemistry, College of Chemistry and Molecular Sciences, Henan University, Kaifeng, Henan 475004, P. R. China

Fax: +86-371-23886876; E-mail for Jingping Wang: jpwang@henu.edu.cn. and E-mail for Jingyang Niu: jyniu@henu.edu.cn.

Supporting Information

Fig. S7. Polyhedral views of the 3D stacking for **1a** along the *c*(a), *b*(b), and *a*(c) axis.
Fig. S8. Nyquist plots of **1** under different RHs at 25 °C.
Fig. S9. The post-proton conduction, experimental, and simulated PXRD patterns of **1**.
Fig. S10. TG curve of **1**.
Fig. S11. IR spectra of **1** and $K_8[Ta_6O_{19}]\cdot 17H_2O$ (**Ta_6**).

Materials and Methods. All other chemicals were commercially purchased and used without further purification. The potassium salt of the $K_8[Ta_6O_{19}]\cdot 17H_2O$ precursor was synthesized according to the reported literature and confirmed by IR spectrum.[S1] IR spectra of all compounds were recorded on a Bruker VERTEX 70 IR spectrometer using KBr pellets in the range of 4000–500 cm^{-1}. Thermogravimetric analysis (TGA) analyses were performed on a NETZSCH STA 449 F5 Jupiter thermal analyzer in flowing N_2 with a heating rate of 10 °C min^{-1}. Powder X-ray diffraction (PXRD) data were performed on an X-ray powder diffractometer (Bruker, D8 Advance) using Cu Kα radiation (λ = 1.5418 Å) collected with the angular range (2θ) from 5° to 45° at room temperature. The proton conduction data was collected by impedance phase gain analyzers Solartron 1260 and 1296. ICP analyses were performed on a PerkinElmer Optima 2000 ICP-OES spectrometer. XPS spectra were measured on Thermo Scientific K-Alpha.

Synthesis

Syntheses of $K_{12}Na_{14}H_{7.4}[Fe_{10.7}Ta_{1.3}O_8(OH)_8(H_2O)_2(Ta_6O_{19})_6]\cdot 114.5H_2O$ (1). 2.01 g of $K_8[Ta_6O_{19}]\cdot 17H_2O$ was dissolved in 150 mL of H_2O. Then, a solution of $FeCl_3\cdot 6H_2O$ (0.405 g, 2.497 mmol) and 1,10-phenanthroline monohydrate (0.595g, 3.002 mmol) with H_2O (5 mL) was added dropwise. After stirring for 20 min, the pH was adjusted to 11.7 with 2 mol/L NaOH, and the reaction was kept at 90 °C for 3 h. The resulting mixture was cooled to room temperature and centrifuged. The orange filtrate was transferred to a straight glass tube, and a mixed solvent of CH_3CH_2OH/H_2O (1:2, volume ratio) was carefully layered onto the orange filtrate. Subsequently, alcohol was carefully layered onto the mixed solvent. Orange block crystals of **1** appeared at the interface after one month (yield: 0.3 % based on Ta). IR (KBr pellets, cm^{-1}): 3357 (br), 1646 (s), 917 (s), 865 (s), 759 (w), 709 (s), 548 (s).

Synthesis discussion

Our initial idea is that organic ligands are added to the reaction system to protect the transition

metals from hydrolysis. Thus, $FeCl_3 \cdot 6H_2O$ and 1,10-phenanthroline were dissolved in an aqueous solution, firstly. Then, the solution is added dropwise to the $K_8[Ta_6O_{19}] \cdot 17H_2O$ solution. We also tried to synthesize compound **1** without 1,10-phenanthroline ligands, however, the amorphous products were formed. The results indicated that 1,10-phenanthroline acts as base coordinate with transition metal ions to prevent them from being hydrolysis. The experiments reveal that the crystals weren't gained if the 1,10-phenanthroline ligands were replaced by other organic ligands (e.g. 2,2'-bipyridine, 4,4-bipyridine) under the same reaction conditions (including the pH values, the the proportion of organic ligands, transition metals and $K_8[Ta_6O_{19}] \cdot 17H_2O$). This may be due to the presence of factors such as the pH of the solution, the proportion of organic ligands, transition metals and $K_8[Ta_6O_{19}] \cdot 17H_2O$. Notably, 1,10-phenanthroline monohydrate ligands are essential for the formation of **1**, although it does not appear in the structure. The similar phenomenon had often been described in previously reported literatures.[S2]

X-ray crystallographic. The suitable single crystal of compound **1** was sticked to the loop for data collection at 150 K. Indexing and data collection were performed on a Bruker D8 VENTURE PHOTON II diffractometer with Mo Kα radiation (λ = 0.71073 Å). Direct methods successfully located the tungsten atoms, and successive Fourier syntheses revealed the remaining atoms. Refinements were done by full-matrix least-squares on F^2 using the SHELXL-2018 program suite for all data.[S3] In the final refinement, all the non-hydrogen atoms were refined anisotropically. The lattice water molecules were located by using a Fourier map. Some hydrogen atoms on partial water molecules were added, and the rest were directly included in the molecular formula. In addition, the partially occupied Ta19 (0.65) and Fe6 (0.35) atoms are assigned in the final refinement.

Proton conduction experiments: AC impedance measurements were performed on Solartron Analytical ModuLab 1260/1296 over the frequency ranging from 1 Hz to 10 MHz. The relative humidity was controlled by a STIK Corp CIHI-150BS3 incubator. The samples were pressed to form a cylindrical pellet of crystalline powder sample (~1 mm thickness × 3 mm diameter). Two silver electrodes were attached to both sides of the pellet to form four end terminals (quasi-four-probe method). Each humidity equilibrium and the thermal equilibrium were kept for 1.5 h. The ZsimpWin software was used to fit the equivalent circuit of the impedance data. The proton conductivity (σ) and activation energy (Ea) were calculated by the two following equations:

$\sigma = d/RS$ (1)

$\sigma T = \sigma_0 \exp(-Ea/K_B T)$ (2)

where d is the thickness (cm) of the slice, S is the electrode area (cm^2), R is the resistance (Ω), σ_0 is the pre-exponential factor, T represents the absolute temperature, and K_B is the Boltzmann constant ($K_B = 8.63 \times 10^{-5}$ eV/K).

Table S1. Summary of all-inorganic Fe^{3+}/Fe^{2+} contain polyanions.

No.	Year	Compounds	Ref.
Fe_{48}	2020	$K_{36}[Fe_{48}(OH)_{76}(H_2O)_{16}(HP_2W_{12}O_{48})_8]\cdot 400H_2O$	S4
Fe_{28}	2005	$Na_{16}K_{12}[H_{56}P_8W_{48}Fe_{28}O_{248}]\cdot ca.90H_2O$	S5
Fe_{18}	2011	$(NH_4)_{12}Cu(H_2O)_4[As_2Fe_6Mo_{22}O_{85}(H_2O)]_3\cdot 20H_2O$	S6
Fe_{16}	2008	$Li_4K_{16}[P_8W_{48}O_{184}Fe_{16}(OH)_{28}(H_2O)_4]\cdot 66H_2O\cdot 2KCl$	S7
		$Na_9K_{11}[P_8W_{48}O_{184}Fe_{16}(OH)_{28}(H_2O)_4]\cdot 100H_2O$	
Fe_{15}	2021	$Na_{21}[NaFe_{15}(OH)_{12}(PO_4)_4(A\text{-}\alpha\text{-}SiW_9O_{34})_4]\cdot 85H_2O$	S8
Fe_{14}	2015	$(CH_6N_3)Na_{30}[Fe_{14}O_6(OH)_{13}(P_2W_{15}O_{56})_4]\cdot 105H_2O\cdot 2NaCH_3COO$	S9
		$Cs_{4.5}K_{14}Na_{1.5}[Na_2Fe_{14}(OH)_{12}(PO_4)_4(A\text{-}\alpha\text{-}SiW_9O_{34})_4]\cdot 105H_2O\cdot 2Na_3PO_4$	
		$Rb_4Na_{16}[Na_2Fe_{14}(OH)_{12}(PO_4)_4(A\text{-}\alpha\text{-}GeW_9O_{34})_4]\cdot 139H_2O\cdot 2Na_3PO_4$	
	2016	$[H_3Rb_3Fe_{14}(OH)_{12}(PO_4)_6(B\text{-}a\text{-}PW_9O_{34})_2]\cdot 21H_2O$	S10
Fe_{13}	2009	$K_8Na_{14}[HMTA]_4[(Fe^{III}_3Fe^{II}_{0.25}(OH)_3)(AsO_4)(AsW_9O_{34})]_4\cdot 24H_2O$	S11
Fe_{12}	2008	$(C_2N_2H_{10})_{11}[\{(B\text{-}\alpha\text{-}PW_9O_{34})Fe_3(OH)_3\}_4(PO_4)_4Fe]\cdot 38H_2O$	S12
Fe_{12}	2007	$K_{21}Na_8[KFe_{12}(OH)_{18}(\alpha\text{-}1,2,3\text{-}P_2W_{15}O_{56})_4]\cdot 70H_2O$	S13
Fe_{11}	2015	$Na_{27}[Fe_{11}(H_2O)_{14}(OH)_2(W_3O_{10})_2(\alpha\text{-}SbW_9O_{33})_6]\cdot 103H_2O$	S14
Fe_{10}	2014	$(NH_4)_9Na_{19}[Fe_{10}Se_8W_{62}O_{222}(OH)_{18}(H_2O)_4]\cdot 42H_2O$	S15
	2016	$[Rb_9Cs_4H_{37}Fe_{10}O_{34}(A\text{-}a\text{-}PW9O_{31})_3(OH)_3]\cdot 36H_2O$	S10
Fe_9	2010	$[EMIM]_8Na_9[WFe_9(\mu_3\text{-}O)_3(\mu_2\text{-}OH)_6O_4H_2O(SiW_9O_{34})_3]\cdot 7H_2O$	S16
Fe_8	2022	$Li_{48}[(Nb_6O_{19})_8Fe_8(OH)_8]\cdot 88H_2O$	S17
	2005	$Na_{10}K_6[H_{12}P_4W_{28}Fe_8O_{120}]\cdot 28H_2O$	S18
	2008	$K_4(C_2N_2H_{10})_{12}[(\alpha\text{-}PW_{10}Fe_2O_{39})_4]\cdot 30H_2O$	S12
Fe_6	2018	$(NH_4)_{25}[As_6Fe_7Mo_{22}O_{98}]\cdot 13H_2O$	S19
	1994	$Na_3(NH_4)_{12}[Mo_{57}Fe_6(NO)_6O_{174}(OH)_3(H_2O)_2]\cdot 76H_2O$	S20
	2005	$Cs_4Na_7[Fe_6(OH)_3(A\text{-}\alpha\text{-}GeW_9O_{34}(OH)_3)_2]\cdot 30H_2O$	S21
	2006	$K_7[(CH_3)_2(NH_2)]_8[\{Fe_2(OH)_3(H_2O)_2\}_3(\gamma\text{-}SiW_{10}O_{36})_3]\cdot 31H_2O$	S22
	2009	$(H_2en)_{2.5}H_9[Fe_6Ge_3W_{24}O_{94}(H_2O)_2]\cdot 14H_2O$	S23
	2012	$(NH_4)_{16}[As_2Fe_6Mo_{20}O_{80}(H_2O)_2]\cdot 18H_2O$	S24
	2013	$[dapH_2]_5[Fe_4(H_2O)_2(FeW_9O_{34})_2]\cdot 11H_2O$	S25
		$[dapH_2]_3[enH_2][enH]Na[Fe_4(H_2O)_2(FeW_9O_{34})_2]\cdot 7H_2O$	

	2014	$(C_2H_8N)_4Na_{14}[Fe_6Se_6W_{34}O_{124}(OH)_{16}]\cdot 44H_2O$	S15
Fe_5	2012	$(NH_4)_{17}[As_2Fe_5Mo_{21}O_{82}]\cdot 14H_2O$	S24
Fe_4	2000	$Rb_{12}(SiW_{10}O_{37})_2Fe_4(OH)_4\cdot 28H_2O$	S26
	2002	$Na_6[Fe_4(H_2O)_{10}(\beta\text{-}AsW_9O_{33})_2]\cdot 32H_2O$	S27
		$Na_6[Fe_4(H_2O)_{10}(\beta\text{-}SbW_9O_{33})_2]\cdot 32H_2O$	
		$Cs_4[Fe_4(H_2O)_{10}(\beta\text{-}SeW_9O_{33})_2]\cdot 21H_2O$	
		$Cs_{3.8}K_{0.2}[Fe_4(H_2O)_{10}(\beta\text{-}TeW_9O_{33})_2]$	
	2007	$K_{14}[\alpha\text{-}GeFe_2W_{10}O_{38}(OH)]_2\cdot 34H_2O$	S28
	2007	$Na_6[Fe_4(H_2O)_{10}(\beta\text{-}AsW_9O_{33})_2]\cdot 32H_2O$	S29
		$Na_6[Fe_4(H_2O)_{10}(\beta\text{-}SbW_9O_{33})_2]\cdot 32H_2O$	
		$Cs_4[Fe_4(H_2O)_{10}(\beta\text{-}SeW_9O_{33})_2]\cdot 21H_2O$	
		$Cs_{3.8}K_{00.2}[Fe_4(H_2O)_{10}(\beta\text{-}TeW_9O_{33})_2]\cdot 32H_2O$	
	2008	$[enH_2]_3[Fe^{III}{}_4(H_2O)_8(SbW_9O_{33})_2]\cdot 20H_2O$	S30
	2020	$(H_2btp)_4[Fe^{III}{}_2Fe^{II}{}_2(H_2O)_2(AsW_9O_{34})_2]\cdot 4H_2O$	S31
	2006	$Rb_{11}[\{(\beta\text{-}SiFe_2W_{10}O_{37}(OH)(H_2O)\}_2(\mu\text{-}OH)]\cdot 20H_2O\cdot 0.5RbCl$	S22
Fe_3	2001	$Na_9[Fe_3(H_2O)_3(BiW_9O_{33})_2]\cdot 37H_2O$	S32
	2002	$\alpha\text{-}Na_{11}[(FeCl)_2(FeOH_2)P_2W_{15}O_{59}]\cdot 14H_2O$	S33
		$\alpha\text{-}Na_9[(FeOH_2)_3P_2W_{15}O_{59}]\cdot 19H_2O$	
		$Na_{14}[\alpha\alpha\beta\alpha\text{-}(NaOH_2)(FeOH_2)Fe_2(P_2W_{15}O_{56})_2]\cdot 20H_2O$	
		$[(CH_3CH_2CH_2CH_2)_4N]_{15}[\alpha\alpha\beta\alpha\text{-}Fe_3(P_2W_{15}O_{56})_2]$	
	2003	$\alpha\beta\beta\alpha\text{-}Na_{12}(Fe^{III}OH_2)_2Fe^{III}{}_2(As_2W_{15}O_{56})_2$	S34
	2003	$\alpha\alpha\beta\alpha\text{-}Na_{14}[(NaOH_2)(Fe^{III}OH_2)(Fe^{III})_2(P_2W_{15}O_{56})_2]$	S35
		$\alpha\alpha\beta\alpha\text{-}Na_{14}[(NaOH_2)(Fe^{III}OH_2)(Fe^{III})_2(As_2W_{15}O_{56})_2]$	
	2004	$K_9[(Fe^{III}(OH_2)_2)_3(A\text{-}\alpha\text{-}PW_9O_{34})_2]$	S36
	2004	$K_4Na_7[(\alpha\text{-}SiFe_3W_9(OH)_3O_{34})_2(OH)_3]$	S37
		$K_2Na_6[(\alpha\text{-}Si(FeOH_2)_2FeW_9(OH)_3O_{34})_2]$	
	2005	$K_4Na_7[(\beta\text{-}SiFe_3W_9(OH)_3O_{34})_2(OH)_3]$	S38
Fe_2	2001	$H_2Na_{14}[Fe^{III}{}_2(NaOH_2)_2(P_2W_{15}O_{56})_2]$	S39
	2007	$Cs_3K_9[K(H_2O)(\beta\text{-}Fe_2GeW_{10}O_{37}(OH))(\gamma\text{-}GeW_{10}O_{36})]\cdot 19H_2O$	S40
		$Cs_7K_4Na[\{\beta\text{-}Fe_2GeW_{10}O_{37}(OH)_2\}_2]\cdot 39H_2O$	
	2008	$K_8[(CH_3)_2NH_2]_5[(\beta\text{-}SiFe_2W_{10}O_{37}(OH))(\gamma\text{-}SiW_{10}O_{36})]\cdot 17H_2O$	S41
	2009	$(NH_4)_{12}[Fe_2(AsMo_7O_{27})_2]\cdot 12H_2O$	S42
	2012	$Fe(H_2O)_6H[Na_6FeW_{12}O_{40}]_2\cdot 44H_2O$	S43
	2016	$Cs_3K_4H_2[(Si_2W_{18}Ta_6O_{78})FeCl_2(H_2O)_2]\cdot 15H_2O$	S44
	2016	$[Fe_2(AsMo_7O_{27})_2](H_2en)_2(NH_4)_8\cdot 6H_2O$	S45
	2017	$Na_{16}[(NaOH_2)_2Fe^{III}{}_2(As_2W_{15}O_{56})_2]\cdot 54H_2O$	S46

	2020	$(H_2bpp)_2[Na_4Fe(H_2O)_7][Fe(P_4Mo_6O_{31}H_6)_2]\cdot 2H_2O$	S47
		$(H_2bpp)_6(bpp)_2[Fe(P_4Mo_6O_{31}H_8)_2]_2\cdot 13H_2O$	
	2003	αααα-$H_2Na_{14}[(NaOH_2)_2Fe^{III}_2(As_2W_{15}O_{56})_2]$	S35
Fe	2020	$[C_{16}H_{33}(CH_3)_3N]_{10}[(PW_{11}FeO_{39})_2O]\cdot 3.5H_2O$	S48
		$[(C_2H_5)_4N]_{10}[(PW_{11}FeO_{39})_2O]\cdot 3H_2O$	
		$[(CH_3)_4N]_{10}[(PW_{11}FeO_{39})_2O]\cdot 4H_2O$	

Table S2. Summary of POTas with transition metals and corresponding synthetic methods.

No.	Compounds	Synthetic method	Reagents and Precursor	Ref.
1	$K_7[Re(CO)_3Ta_6O_{19}]$	Reflux 60 °C for 2.5 h under N_2	$[Re(CO)_3(CH_3CN)_3]ClO_4$ $K_8[Ta_6O_{19}]\cdot 17H_2O$	S49
2	$K_7[Mn(CO)_3Ta_6O_{19}]$	Reflux 60 °C for 2.5 h under N_2	$[Mn(CO)_3(CH_3CN)_3]ClO_4$ $K_8[Ta_6O_{19}]\cdot 17H_2O$	S49
3	*cis*-$K_6[\{Mn(CO)_3\}_2Ta_6O_{19}]$	Reflux 100 °C for 2 h	$[Mn(CO)_3(CH_3CN)_3]ClO_4$ $K_8[Ta_6O_{19}]\cdot 17H_2O$	S49
4	*trans*-$K_4Na_2[\{Re(CO)_3\}_2Ta_6O_{19}]$	Reflux 100 °C for 1 h	$[Re(CO)_3(CH_3CN)_3]ClO_4$ $K_8[Ta_6O_{19}]\cdot 17H_2O$	S49
5	$\{[Cu(1,3\text{-dap})_2]_2[Cu(1,3\text{-dap})(H_2O)]_2[Ta_6O_{19}]\}\cdot 8H_2O$	Diffusion	CuI, pyrazine, 1,3-dap $K_8[Ta_6O_{19}]\cdot 17H_2O$	S50
6	$[Cu(en)_2]_4[Ta_6O_{19}]\cdot 14H_2O$	Diffusion	$Cu(CH_3COOH)_2\cdot H_2O$, en $K_8[Ta_6O_{19}]\cdot 17H_2O$	S50
7	$Na_{10}[\{(C_6H_6)RuTa_6O_{18}\}_2(\mu\text{-}O)]\cdot 39.4H_2O$	80 °C for 8 h	$[(C_6H_6)RuCl_2]_2$ $Na_8[Ta_6O_{19}]\cdot 24.5H_2O$	S51
8	$Na_4(trans\text{-}[\{(C_6H_6)Ru\}_2Ta_6O_{19}]\cdot 20H_2O$	80 °C for 8 h	$[(C_6H_6)RuCl_2]_2$ $Na_8[Ta_6O_{19}]\cdot 24.5H_2O$	S51
9	$Cs_4[(Cp^*Rh)_2Ta_6O_{19}]\cdot 18H_2O$	80 °C for 8 h	$[Cp^*RhCl_2]_2$ $Cs_8[Ta_6O_{19}]\cdot 14H_2O$	S52
10	$TMA_8Ti_2Ta_8O_{28}\cdot 21H_2O$	Hydrothermal (140°C for 16 h), postprocessing	$TMAOH\cdot 5H_2O$, $Ti\{OCH(CH_3)_2\}_4$, $Ta_2O_5\cdot nH_2O$	S53
11	$TMA_{10}Ti_{12}Ta_6O_{44}\cdot 39H_2O$	Hydrothermal (150°C for 16 h), postprocessing	$TMAOH\cdot 5H_2O$, $Ti\{OCH(CH_3)_2\}_4$, $Ta_2O_5\cdot nH_2O$	S53
12	$Na_6[\{Cp^*Ir\}Ta_6O_{19}]\cdot 27H_2O$	60 °C for 48 h	$[Cp^*IrCl_2]_2$ $Na_8[Ta_6O_{19}]\cdot 24.5H_2O$	S54
13	$Na_4[\{Cp^*Ir\}_2Ta_6O_{19}]\cdot 24H_2O$	60 °C for 48 h	$[Cp^*IrCl_2]_2$ $Na_8[Ta_6O_{19}]\cdot 24.5H_2O$	S54
14	$Na_4[trans\text{-}\{Cp^*Rh\}_2Ta_6O_{19}]\cdot 24H_2O$	80°C for 24 h	$[Cp^*RhCl_2]_2$ $Na_8[Ta_6O_{19}]\cdot 24.5H_2O$	S55

15	$Na_8K_7[(Ta_6O_{19})_4H_5Co_8O_4]\cdot 45H_2O$	90 °C for 3 h	$CoCl_2\cdot 6H_2O$ $K_8[Ta_6O_{19}]\cdot 17H_2O$	S56
16	$Na_4(NH_4)_2[(Ta_6O_{19})Co(H_2O)_3]\cdot 20H_2O$	90 °C for 3 h	$CoCl_2\cdot 6H_2O$, NH_3 $K_8[Ta_6O_{19}]\cdot 17H_2O$	S57
17	$Na_4K_6[(Ta_6O_{19})Co(en)]_2\cdot 30H_2O$	90 °C for 3 h	$CoCl_2\cdot 6H_2O$, en $K_8[Ta_6O_{19}]\cdot 17H_2O$	S57
18	$\{[CuL]_2[CuL_2]_2[Ta_6O_{19}]\}\cdot 21H_2O$	60 °C for 8 h	$Na_4P_2O_7$, 1,10-phen, $Cu(NO_3)_2\cdot 3H_2O$, $K_8[Ta_6O_{19}]\cdot 17H_2O$	S58
19	$\{[CuL']_2[CuL'_2]_2[Ta_6O_{19}]\}\cdot 20H_2O$	60 °C for 8 h	$Na_4P_2O_7$, 2,2'-bipy, $Cu(NO_3)_2\cdot 3H_2O$, $K_8[Ta_6O_{19}]\cdot 17H_2O$	S58
20	$H_2[Cu(en)_2(H_2O)_2]\{[Cu(en)_2]_4[Cu(en)(Ta_6O_{19})]_2\}\cdot 14H_2O$	Hydrothermal (100 °C for 3 days)	$Na_8[Ta_6O_{19}]\cdot 24.5H_2O$, $CrCl_3\cdot 6H_2O$, CuSCN, $C_4H_8O_2$, en, $Na_8[Ta_6O_{19}]\cdot 24.5H_2O$	S57
21	$H_2\{[Cu(en)_2]_3[Cu(en)(H_2O)_2Cu(en)(Ta_6O_{19})]_2\}\cdot 30H_2O$	Structural transformations triggered by water	$H_2[Cu(en)_2(H_2O)_2]\{[Cu(en)_2]_4[Cu(en)(Ta_6O_{19})]_2\}\cdot 14H_2O$	S59
22	$H_2[Cu(enMe)_2(H_2O)_2][Na_2(H_2O)_{10}]_2\{[Cu(enMe)_2]_2[Cu(enMe)(Ta_6O_{19})]_2\}\cdot 26H_2O$	Hydrothermal (100 °C for 3 days)	$CrCl_3\cdot 6H_2O$, CuSCN, $C_4H_8O_2$, enMe, $Na_8[Ta_6O_{19}]\cdot 24.5H_2O$	S59
23	$H_4[Na_4(H_2O)_{18}]\{[Cu(enMe)_2]_2[Cu(enMe)(Ta_6O_{19})]_2\}\cdot 10H_2O$	Structural transformations triggered by water	$H_2[Cu(enMe)_2(H_2O)_2][Na_2(H_2O)_{10}]_2\{[Cu(enMe)_2]_2[Cu(enMe)(Ta_6O_{19})]_2\}\cdot 26H_2O$	S59
24	$H_2[Cu(en)_2(H_2O)_2]\{[Cu(en)_2]_2[Na_2(H_2O)_7]_2[Cu(en)(Ta_6O_{19})]_2\}\cdot 10H_2O$	Hydrothermal (100 °C for 3 days)	$CrCl_3\cdot 6H_2O$, $Na_2MoO_4\cdot 2H_2O$, CuSCN, $C_4H_8O_2$, en, $Na_8[Ta_6O_{19}]\cdot 24.5H_2O$	S59
25	$H_2[Na_2(H_2O)_{10}]_2[Cu(en)_2]_2\{[Cu(en)_2][Cu(en)(Ta_6O_{19})]_2\}\cdot 8H_2O$	Hydrothermal (100 °C for 3 days)	$CrCl_3\cdot 6H_2O$, $NaBO_3\cdot 4H_2O$, CuSCN $NaCO_3/NaHCO_3$ (0.5M, pH=10.5) buffer solution, en, $Na_8[Ta_6O_{19}]\cdot 24.5H_2O$	S59
26	$K_4\{[Cu(cyclam)]_2Ta_6O_{19}\}\cdot 18H_2O$	Diffusion	$Cu(NO_3)_2\cdot 3H_2O$, cyclam, $K_8\{Ta_6O_{19}\}\cdot 16H_2O$	S60
27	$K_4\{[Zn(cyclam)]_2Ta_6O_{19}\}\cdot 18H_2O$	Diffusion	$Zn(NO_3)_2\cdot 6H_2O$, cyclam, $K_8\{Ta_6O_{19}\}\cdot 16H_2O$	S60
28	$\{[Cd(cyclam)]_4Ta_6O_{19}\}\cdot 19H_2O$	Diffusion	$Cd(NO_3)_2\cdot 4H_2O$, cyclam, $K_8\{Ta_6O_{19}\}\cdot 16H_2O$	S60

1,3-dap=1,3-diaminopropane,[S50] en=ethylenediamine; [S50, S57, S59] Cp* = η_5-$C_5(CH_3)_5$);[S54] L = 1,10-phen;[S58] L′ = 2,2′-bipy;[S58] enMe = 1,2-diaminopropane;[S59] $C_4H_8O_2$ = 1,4-dioxane;[S59] cyclam=1,4,8,11-tetraazacyclotetradecane;[S60]

Table S3. Crystallographic data and structure refinements for **1**.

	1
Empirical formula	$K_{12}Na_{14}H_{248.4}Fe_{10.7}Ta_{37.3}O_{246.5}$
Formula weight	12332.47
Temperature / K	150
Crystal system	triclinic
Space group	*P*-1
a [Å]	18.011(18)
b [Å]	19.645(19)
c [Å]	20.630(17)
α [°]	113.52(2)
β [°]	94.90(2)
γ [°]	113.32(3)
V [Å^3]	5883(9)
Z	1
ρ_{calcd} [g cm^{-3}]	3.481
μ [mm^{-1}]	18.260
F(000)	5604.0
Index ranges	$-21 \le h \le 21$ $-23 \le k \le 23$ $-24 \le l \le 24$
Reflections collected	127309
Independent reflections	21832 [R_{int} = 0.0504]
data/restraints/ parameters	21832/193/1435
Goodness-of-fit on F^2	1.012
R_1, wR_2 [$I > 2\sigma(I)$]	0.0282, 0.0595
R_1, wR_2 [all data]	0.0358, 0.0632
Largest diff. Peak/hole/e Å^{-3}	2.52/-1.26

Table S4. BVS values for Fe atoms in **1**.

Atoms	BVS value	Atoms	BVS value	Atoms	BVS value
Fe1	2.89	Fe3	2.87	Fe5	3.09
Fe2	2.80	Fe4	2.82	Fe6	3.19

Table S5. BVS values for O atoms in **1**.

Atoms	BVS value	Atoms	BVS value	Atoms	BVS value
O23	0.98	O47	0.98	O49	0.96
O6	0.97	O1W	0.51		

Table S6. Possible geometries of six coordinated metal centers.

Geometry	Point group	Polyhedron
HP-6	D_{6h}	Hexagon
PPY-6	C_{5v}	Pentagonal pyramid
OC-6	O_h	Octahedron
TPR-6	D_{3h}	Trigonal prism
JPPY-6	C_{5v}	Johnson pentagonal pyramid J2

Table S7. Deviation parameters calculated by SHAPE from each ideal polyhedron for Fe atoms in **1**.

	Fe1	Fe2	Fe3	Fe4	Fe5	Fe6
HP-6	30.567	32.532	31.246	31.536	30.115	32.141
PPY-6	27.823	25.851	24.249	24.915	28.194	28.973
OC-6	0.358	0.500	1.572	1.494	0.854	0.564
TPR-6	15.440	12.202	10.614	10.828	15.681	15.949
JPPY-6	31.468	29.618	27.360	28.120	31.469	32.454

Table S8. Selected bond lengths (Å) of **1**.

Bond	Length	Bond	Length	Bond	Length
Fe1-O4	2.079(6)	Fe3-O3	2.095(6)	Fe5-O1	2.165(6)
Fe1-O9	2.087(6)	Fe3-O14	2.146(6)	Fe5-O10	1.828(6)
Fe1-O10	1.929(6)	Fe3-O20	1.972(6)	Fe5-O46	2.085(6)
Fe1-O10	2.012(6)	Fe3-O23	1.993(6)	Fe5-O48	2.080(6)
Fe1-O47	2.040(6)	Fe3-O45	2.124(6)	Fe5-O50	1.979(6)
Fe1-O49	2.051(6)	Fe3-O53	1.923(6)	Fe5-O53	1.986(6)
Fe2-O6	2.061(6)	Fe4-O2	2.107(6)	Fe6-O1W	2.353(6)
Fe2-O23	2.055(6)	Fe4-O6	1.998(6)	Fe6-O9	1.831(6)
Fe2-O24	2.055(6)	Fe4-O8	2.113(6)	Fe6-O27	2.023(6)
Fe2-O47	2.008(6)	Fe4-O21	2.012(6)	Fe6-O50	1.960(6)
Fe2-O49	2.011(6)	Fe4-O50	1.923(6)	Fe6-O53	1.964(6)
Fe2-O61	2.060(6)	Fe4-O59	2.113(6)	Fe6-O60	2.003(6)

Table S9. Bond angles (°) for the central $\{Fe_{10.7}Ta_{1.3}O_8(OH)_8(H_2O)_2\}$ fragment in **1**.

Bond	Angle	Bond	Angle
Fe4-O6-Fe2	131.7(3)	Fe4-O50-Fe6	139.9(3)
Fe6-O9-Fe1	130.9(3)	Fe6-O50-Fe5	95.4(3)
Fe1-O10-Fe1	98.6(3)	Fe3-O53-Fe5	124.4(3)
Fe5-O10-Fe1	126.9(3)	Fe3-O53-Fe6	140.2(3)
Fe5-O10-Fe1	134.5(3)	Fe6-O53-Fe5	95.1(3)
Fe3-O23-Fe2	132.3(3)	Fe2-O49-Fe1	129.9(3)
Fe2-O47-Fe1	130.3(3)	Fe4-O50-Fe5	124.1(3)

Table S10. Data of proton conductivity σ ($S \cdot cm^{-1}$) of **1** at various temperature conditions under 85% RH.

T (℃)	**1**
25	9.24×10^{-4}
35	1.68×10^{-3}
45	2.47×10^{-3}
55	4.29×10^{-3}
65	8.52×10^{-3}
75	1.59×10^{-2}
85	2.61×10^{-2}

Table S11. Calculated and found analyses of Na, K, Ta, and Fe with massic ratios in **1**.

	Na (%)	**K (%)**	**Ta (%)**	**Fe (%)**
calcd	2.61	3.80	54.73	4.85
found	2.65	4.07	59.00	5.13

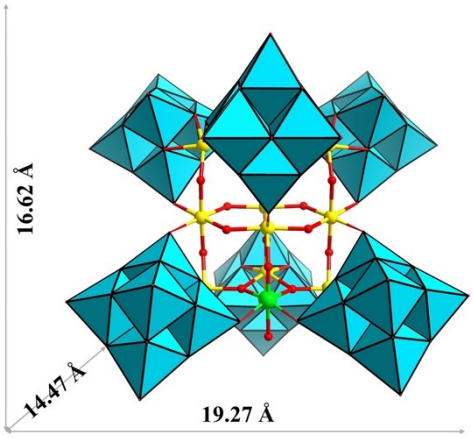

Fig. S1. Representation of polyanion **1a**.

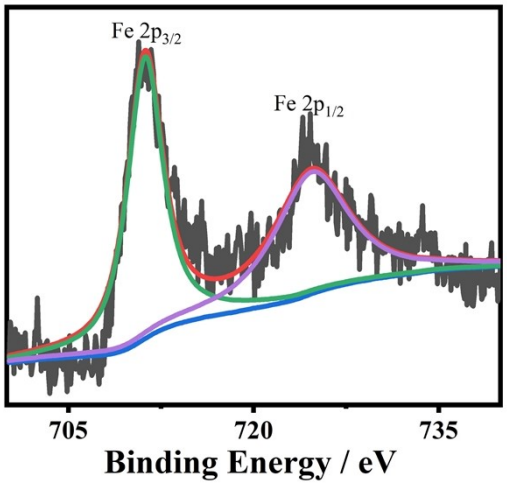

Fig. S2. XPS spectrum of Fe 2p of **1**.

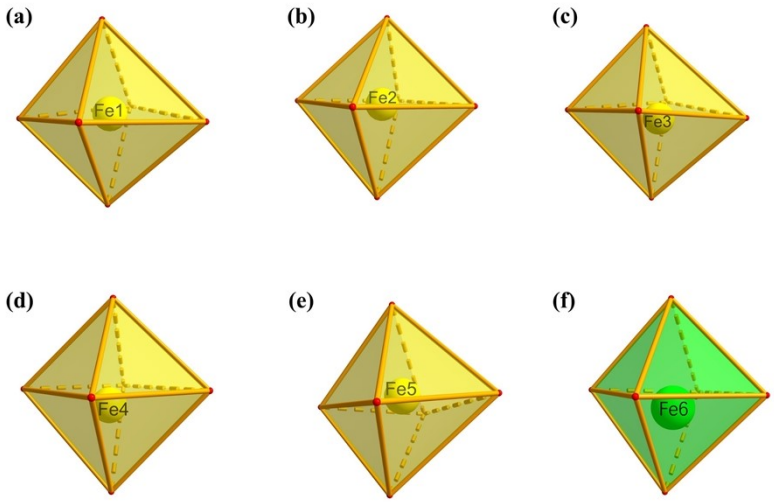

Fig. S3. Geometrical configuration of the Fe^{3+} cations in **1a**.

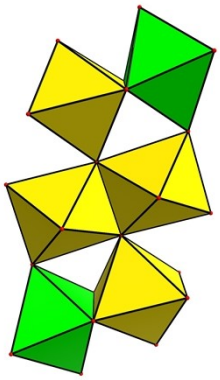

Fig. S4. The polyhedral representation of $\{Fe_{4.7}Ta_{1.3}O_4\}$ core.

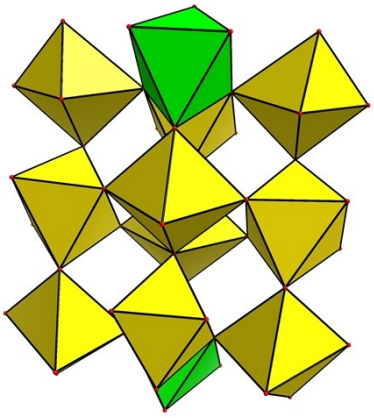

Fig. S5. The polyhedral representation of $\{Fe_{10.7}Ta_{1.3}O_8(OH)_8(H_2O)_2\}$ core.

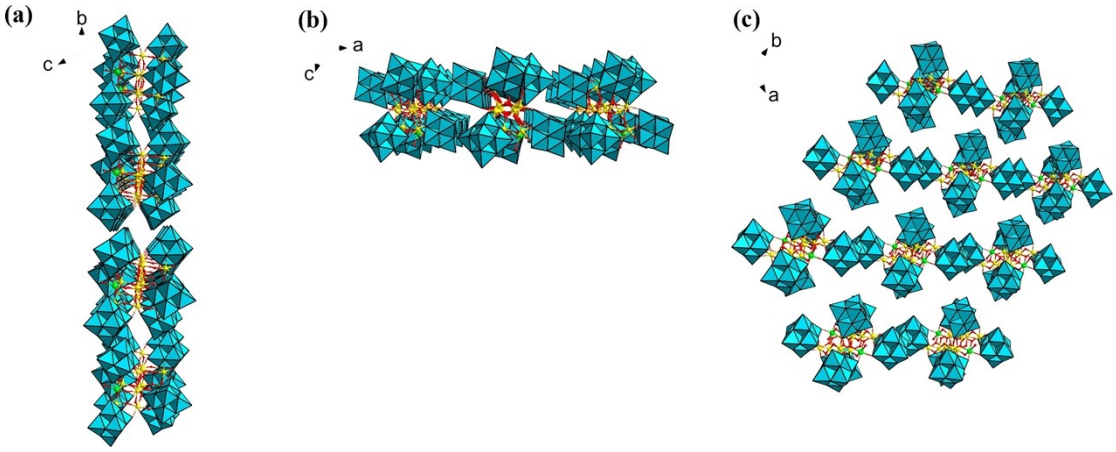

Fig. S6. The packing arrangements of polyoxoanion **1a** along the *a*, *b*, and *c*-axis, respectively.

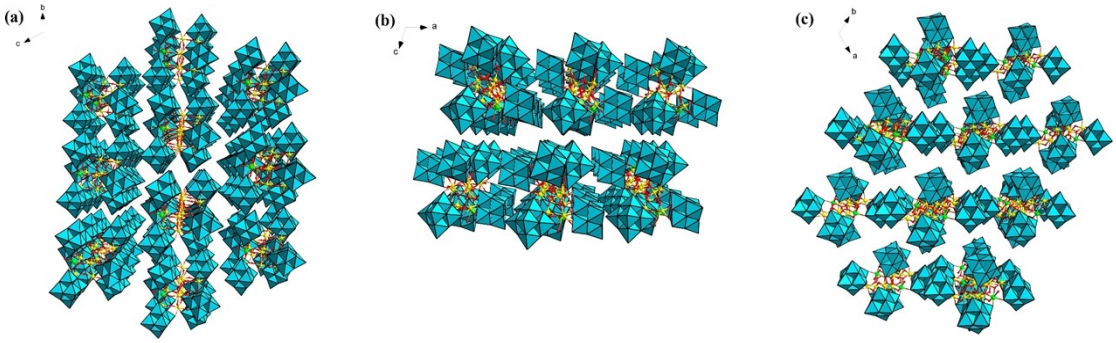

Fig. S7. Polyhedral views of the 3D stacking for **1a** along the *c*(a), *b*(b), and *a*(c) axis.

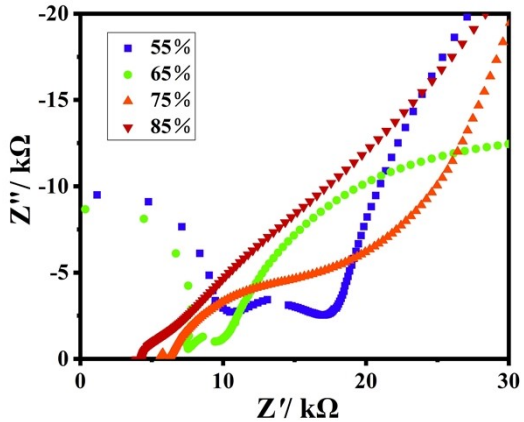

Fig. S8. Nyquist plots of **1** under different RHs at 25 °C.

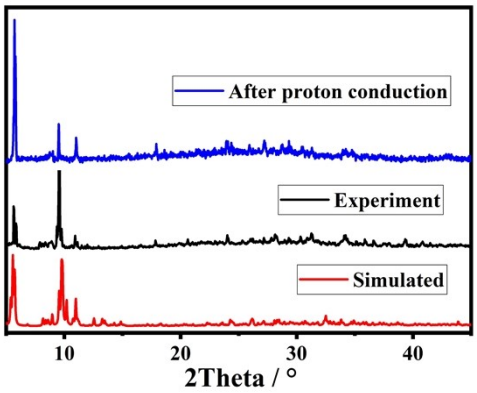

Fig. S9. The post proton conduction, experimental, and simulated PXRD patterns of **1**.

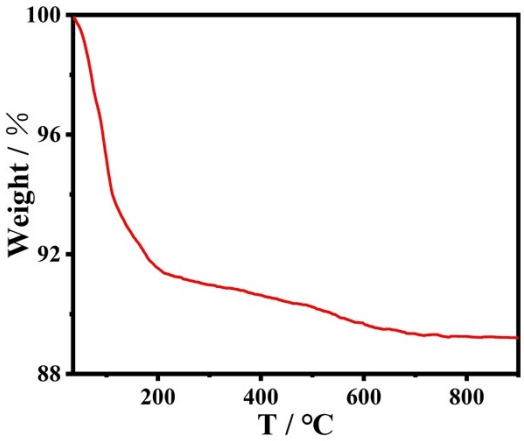

Fig. S10. TG curve of **1**.

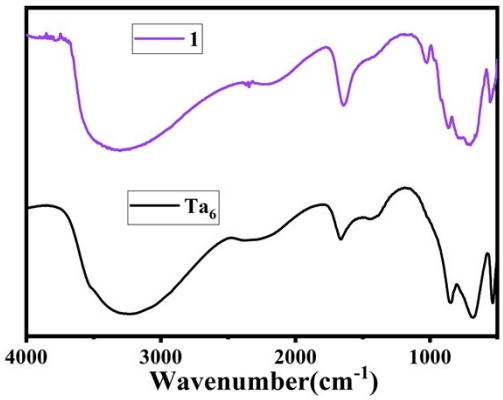

Fig. S11. IR spectra of **1** and $K_8[Ta_6O_{19}]\cdot 17H_2O$ (**Ta_6**).

References

S1 M. Han, Y. Niu, R. Wan, Q. Xu, J. Lu, P. Ma, C. Zhang, J. Niu and J. Wang, *Chem. - Eur. J.*, 2018, **24**, 11059–11066.

S2 J. Niu, F. Li, J. Zhao, P. Ma, D. Zhang, B. Bassil, U. Kortz and J. Wang, *Chem. - Eur. J.*, 2014, **20**, 9852–9857.

S3 G. M. Sheldrick, *Acta Crystallogr. Sect. C Struct. Chem.*, 2015, **71**, 3–8.

S4 J. Goura, B. S. Bassil, J. K. Bindra, I. A. Rutkowska, P. J. Kulesza, N. S. Dalal and U. Kortz, *Chem. – Eur. J.*, 2020, **26**, 15821–15824.

S5 B. Godin, Y.-G. Chen, J. Vaissermann, L. Ruhlmann, M. Verdaguer and P. Gouzerh, *Angew. Chem. Int. Ed.*, 2005, **44**, 3072–3075.

S6 B. Liu, L. Li, Y. Zhang, Y. Ma, H. Hu and G. Xue, *Inorg. Chem.*, 2011, **50**, 9172–9177.

S7 S. S. Mal, M. H. Dickman, U. Kortz, A. M. Todea, A. Merca, H. Bögge, T. Glaser, A. Müller, S. Nellutla, N. Kaur, J. van Tol, N. S. Dalal, B. Keita and L. Nadjo, *Chem. - Eur. J.*, 2008, **14**, 1186–1195.

S8 T. Cui, L. Qin, F. Fu, X. Xin, H. Li, X. Fang and H. Lv, *Inorg. Chem.*, 2021, **60**, 4124–4132.

S9 M. Ibrahim, A. Haider, Y. Xiang, B. S. Bassil, A. M. Carey, L. Rullik, G. B. Jameson, F. Doungmene, I. M. Mbomekallé, P. de Oliveira, V. Mereacre, G. E. Kostakis, A. K. Powell and U. Kortz, *Inorg. Chem.*, 2015, **54**, 6136–6146.

S10 V. Singh, Z. Chen, P. Ma, D. Zhang, M. G. B. Drew, J. Niu and J. Wang, *Chem. - Eur. J.*, 2016, **22**, 10983–10989.

S11 W. Chen, Y. Li, Y. Wang, E. Wang and Z. Zhang, *Z. Für Anorg. Allg. Chem.*, 2009, **635**, 1678–1687.

S12 C. Pichon, A. Dolbecq, P. Mialane, J. Marrot, E. Rivière and F. Sécheresse, *Dalton Trans*, 2008, 71–76.

S13 C. P. Pradeep, D.-L. Long, P. Kögerler and L. Cronin, *Chem. Commun.*, 2007, 4254–4256.

S14 X. Du, J. Zhao, J. Mi, Y. Ding, P. Zhou, B. Ma, J. Zhao and J. Song, *Nano Energy*, 2015, **16**, 247–255.

S15 W.-C. Chen, C. Qin, X.-L. Wang, Y.-G. Li, H.-Y. Zang, P. Huang, K.-Z. Shao, Z.-M. Su and E.-B. Wang, *Chem Commun*, 2014, **50**, 13265–13267.

S16 S. Lin, W. Liu, Y. Li, Q. Wu, E. Wang and Z. Zhang, *Dalton Trans*, 2010, **39**, 1740–1744.

S17 M. Baranov, L. Polin, N. Leffler, G. Leitus, A. I. Shames and I. A. Weinstock, *Dalton Trans.*, 2022, **51**, 8600–8604.

S18 B. Godin, J. Vaissermann, P. Herson, L. Ruhlmann, M. Verdaguer and P. Gouzerh, *Chem. Commun.*, 2005, 5624–5626.

S19 P. Wu, Y. Zhang, C. Feng, B. Liu, H. Hu and G. Xue, *Dalton Trans.*, 2018, **47**, 15661–15665.

S20 A. Miiller, W. Plass, E. Krickemeyer, S. Dillinger, C. Beugholt and U. Bergmann, *Monatshefte Ffir Chem.*, 1994, **125**, 525–533.

S21 L.-H. Bi, U. Kortz, S. Nellutla, A. C. Stowe, J. van Tol, N. S. Dalal, B. Keita and L. Nadjo, *Inorg. Chem.*, 2005, **44**, 896–903.

S22 B. Botar, Y. V. Geletii, P. Kögerler, D. G. Musaev, K. Morokuma, I. A. Weinstock and C. L. Hill, *J. Am. Chem. Soc.*, 2006, **128**, 11268–11277.

S23 B. Li, J.-W. Zhao, S.-T. Zheng and G.-Y. Yang, *Inorg. Chem. Commun.*, 2009, **12**, 69–71.

S24 X. Dong, Y. Zhang, B. Liu, Y. Zhen, H. Hu and G. Xue, *Inorg. Chem.*, 2012, **51**, 2318–2324.

S25 D. Zhang, C. Wang, S. Li, J. Liu, P. Ma, J. Wang and J. Niu, *J. Solid State Chem.*, 2013, **198**, 18–23.

S26 A. Teze and J. Vaissermann, *C R Acad Sci Paris Se´rie IIc Chim. Chem.*, 2000, **3**, 101–105.

S27 U. Kortz, M. G. Savelieff, B. S. Bassil, B. Keita and L. Nadjo, *Inorg. Chem.*, 2002, **41**, 783–789.

S28 Y. Liu, J. Shang, G. Xue, H. Hu, F. Fu and J. Wang, *J. Clust. Sci.*, 2007, **18**, 205–216.

S29 L. Chen, K. Zhu, L.-H. Bi, A. Suchopar, M. Reicke, G. Mathys, H. Jaensch, U. Kortz and R. M. Richards, *Inorg. Chem.*, 2007, **46**, 8457–8459.

S30 A. Dolbecq, J.-D. Compain, P. Mialane, J. Marrot, E. Rivière and F. Sécheresse, *Inorg. Chem.*, 2008, **47**, 3371–3378.

S31 X. Ma, K. Yu, J. Yuan, L. Cui, J. Lv, W. Dai and B. Zhou, *Inorg. Chem.*, 2020, **59**, 5149–5160.

S32 D. Rusu, C. Crăciun, A.-L. Barra, L. David, M. Rusu, C. Roşu, O. Cozar and G. Marcu, *J. Chem. Soc. Dalton Trans.*, 2001, 2879–2887.

S33 T. M. Anderson, X. Zhang, K. I. Hardcastle and C. L. Hill, *Inorg. Chem.*, 2002, **41**, 2477–2488.

S34 I. M. Mbomekalle, B. Keita, L. Nadjo, P. Berthet, K. I. Hardcastle, C. L. Hill and T. M. Anderson, *Inorg. Chem.*, 2003, **42**, 1163–1169.

S35 I. M. Mbomekalle, B. Keita, L. Nadjo, W. A. Neiwert, L. Zhang, K. I. Hardcastle, C. L. Hill and T. M. Anderson, *Eur. J. Inorg. Chem.*, 2003, **2003**, 3924–3928.

S36 N. M. Okun, M. D. Ritorto, T. M. Anderson, R. P. Apkarian and C. L. Hill, *Chem. Mater.*, 2004, **16**, 2551–2558.

S37 T. M. Anderson, W. A. Neiwert, K. I. Hardcastle and C. L. Hill, *Inorg. Chem.*, 2004, **43**, 7353–7358.

S38 T. M. Anderson, R. Cao, W. A. Neiwert, K. I. Hardcastle, C. L. Hill, M. Ammam, B. Keita and L. Nadjo, *Eur. J. Inorg. Chem.*, 2005, **2005**, 1770–1775.

S39 X. Zhang, T. M. Anderson, Q. Chen and C. L. Hill, *Inorg. Chem.*, 2001, **40**, 418–419.

S40 N. H. Nsouli, S. S. Mal, M. H. Dickman, U. Kortz, B. Keita, L. Nadjo and J. M. Clemente-Juan, *Inorg. Chem.*, 2007, **46**, 8763–8770.

S41 B. Botar and P. Kögerler, *Dalton Trans.*, 2008, 3150–3152.

S42 H. Xu, L. Li, B. Liu, G. Xue, H. Hu, F. Fu and J. Wang, *Inorg. Chem.*, 2009, **48**, 10275–10280.

S43 H. H. Wu, Z. M. Zhang and E. B. Wang, *Chin. Chem. Lett.*, 2012, **23**, 355–358.

S44 P. Huang, X.-G. Han, X.-L. Li, C. Qin, X.-L. Wang and Z.-M. Su, *CrystEngComm*, 2016, **18**, 8722–8725.

S45 Q. Wu, X. Miao, H. Wang, Y. Wu, J. Li, J. Lu, Q. Zhou and H. Ju, *Z. Für Naturforschung B*, 2016, **71**, 783–788.

S46 C. S. Ayingone Mezui, P. de Oliveira, A.-L. Teillout, J. Marrot, P. Berthet, M. Lebrini and I. M. Mbomekallé, *Inorg. Chem.*, 2017, **56**, 1999–2012.

S47 X. Xin, N. Hu, Y. Ma, Y. Wang, L. Hou, H. Zhang and Z. Han, *Dalton Trans.*, 2020, **49**, 4570–4577.

S48 Y. Xue, J. Chen, J. Shao, L. Han, W. Li and C. Sui, *Mol. Catal.*, 2020, **492**, 111010.

S49 A. V. Besserguenev, M. H. Dickman and M. T. Pope, *Inorg. Chem.*, 2001, **40**, 2582–2586.

S50 G.-L. Guo, Y.-Q. Xu, B.-K. Chen, Z.-G. Lin and C.-W. Hu, *Inorg. Chem. Commun.*, 2011, **14**, 1448–1451.

S51 P. A. Abramov, M. N. Sokolov, S. Floquet, M. Haouas, F. Taulelle, E. Cadot, E. V. Peresypkina, A. V. Virovets, C. Vicent, N. B. Kompankov, A. A. Zhdanov, O. V. Shuvaeva and V. P. Fedin, *Inorg. Chem.*, 2014, **53**, 12791–12798.

S52 P. A. Abramov, M. N. Sokolov, A. V. Virovets, S. Floquet, M. Haouas, F. Taulelle, E. Cadot, C. Vicent and V. P. Fedin, *Dalton Trans.*, 2015, **44**, 2234–2239.

S53 J. Son and W. H. Casey, *Chem. – Eur. J.*, 2016, **22**, 14155–14157.

S54 P. A. Abramov, C. Vicent, N. B. Kompankov, A. L. Gushchin and M. N. Sokolov, *Eur. J. Inorg. Chem.*, 2016, **2016**, 154–160.

S55 P. A. Abramov, N. B. Kompankov and M. N. Sokolov, *Russ. J. Coord. Chem.*, 2016, **42**, 311–315.

S56 Z. Liang, S. Zhao, P. Ma, C. Zhang, J. Sun, T. Song, J. Niu and J. Wang, *Inorg. Chem.*, 2018, **57**, 12471–12474.

S57 S. Li, S. Chen, F. Zhang, Z. Li, C. Zhang, G. Cao and B. Zhai, *Inorg. Chem. Commun.*, 2019, **106**, 228–232.

S58 Y. Ma, J. Sun, C. Li, N. Li, P. Ma, D. Zhang, G. Wang and J. Niu, *Inorg. Chem. Commun.*, 2019, **101**, 6–10.

S59 Z. Li, J. Zhang, L.-D. Lin, J.-H. Liu, X.-X. Li and S.-T. Zheng, *Chem. Commun.*, 2019, **55**, 11735–11738.

S60 D.-C. Krause, S. Mangelsen, C. Näther and W. Bensch, *Cryst. Growth Des.*, 2021, **21**, 7128–7138.